Evaluation of surface tension of mold fluxes containing fluoride

by J.F. Xu[1], P.W. Gu[1], L.J. Su[1], and J.Y. Zhang[2]

Affiliation:
[1]School of Iron and Steel, Soochow University, Suzhou, China
[2]State Key Laboratory of Advanced Special Steel, Shanghai University, Shanghai, China

Correspondence to:
J.F. Xu

Email:
xujifangsuda@163.com

Dates:
Received: 5 Aug. 2020
Revised: 10 Feb. 2024
Accepted: 15 May 2024
Published: December 2024

How to cite:
Xu, J.F., Gu, P.W., Su, L.J., and Zhang, J.Y. 2024. Evaluation of surface tension of mold fluxes containing fluoride. *Journal of the Southern African Institute of Mining and Metallurgy*, vol. 124, no.12, pp. 755–762

DOI:
http://dx.doi.org/10.17159/2411-9717/1313/2024

ORCiD:
J.F. Xu
http://orcid.org/0000-0002-5753-4041
P.W. Gu
http://orcid.org/0009-0002-6394-1062
L.J. Su
http://orcid.org/0009-0009-1226-2642
J.Y. Zhang
http://orcid.org/0009-0007-5393-1983

Abstract

Surface tension of mold flux is a key factor affecting optimum casting conditions. A thermodynamic model was developed to determine the surface tension of mold flux containing fluoride based on the ion and molecule coexistence theory of slag structure and Butler's equation. The relationship between composition and surface tension was investigated by this model. Results indicated that the calculated values showed good agreement with literature data, and the average error was 8.19%. The surface tension value of the $CaO–Al_2O_3$-based mold flux was larger than that of the $CaO–SiO_2$-based mold flux. The surface tension in a multi-component system decreased with increasing contents of SiO_2, CaF_2, and Na_2O, which are considered surface-active components. This trend was more significant in the $CaO–Al_2O_3$-based mold flux.

Keywords

surface tension, mold flux, fluoride, coexistence theory, model

Introduction

During the continuous casting of steel, the mold flux plays an important role in process performance and product defects, which directly determine the final slab quality (Mills et al., 2005). Typical mold fluxes belong to the conventional $CaO–SiO_2$-based system and the newly developed $CaO–Al_2O_3$-based system. CaF_2, MgO, and Na_2O are added to mold flux to modify its properties (Wang et al., 2016). Although the presence of fluoride in mold flux has been identified as a health hazard and correlated to incidences of cancer, it is still widely used because of its remarkable effect on increasing melting point, viscosity, and surface tension. Knowledge of the surface tension of molten slag is useful for understanding various surface or interfacial phenomena in high-temperature processes. Many metallurgical phenomena are closely related to surface tension (Wang et al., 2016). The surface tension of mold flux is a key factor in achieving optimum casting conditions in a continuous casting process, because it affects the interfacial reaction between the mold flux and steel, the absorption of inclusions, and corrosion of the mold nozzle.

The main interest of this work concerns the surface tension of mold flux containing fluoride. Several prior experimental studies were carried out to determine surface tension data for mold fluxes (Mills et al., 2011; Slag Atlas, 1995); however, due to inherent problems and difficulties associated with measurements at high temperature, calculated results have become increasingly important for acquiring such data. It is necessary to have access to reliable models for estimating surface tension. There are many models for estimating surface tension of molten slag (Aune et al., 2002; Cheng and Liao, 1999; Chou and Zhang, 2009; Dong et al., 2014; Mills et al., 2011; Qiao et al., 2001; Xu et al., 2016; Zhang et al., 2003), most of which are proposed based on the structure of atoms and molecules with a physical picture of the practical solution, or combine theoretical considerations with practical thermodynamics. In the present work, based on the ion and molecule coexistence theory of slag structure and Butler's equation, a new thermodynamic model was developed for determining the surface tension of mold flux containing fluoride. The relationship between the composition and surface tension was also investigated, which helps to understand its performance and provide candidates for the design of new mold fluxes.

Model for estimating surface tension

A model derived for the estimation of surface tension of ionic mixtures was applied to a six-component molten slag in the $CaO–MgO–Al_2O_3–SiO_2–CaF_2–Na_2O$ system, which is a typical mold flux containing fluoride for continuous casting. Based on Butler's equation, the surface tension (σ) of a mold flux containing fluoride is calculated as follows (Butler, 1932):

$$\sigma = \sigma_i^{Pure} + \frac{RT}{A_i} ln \frac{N_i^{Surf}}{N_i^{Bulk}}; \quad [1]$$

where subscript i refers to CaO, MgO, Al_2O_3, SiO_2, CaF_2, or Na_2O in the present work. R is the gas constant, T is the absolute temperature, and $A_i = N_0^{1/3} \cdot V_i^{2/3}$ corresponds to the molar surface area in a monolayer of pure molten component i (N_0 is Avogadro's number, V_i is the molar volume of the pure molten component i). N_i^{Surf} and N_i^{Bulk} are the mass action concentrations (activities) of component i in the surface and bulk, respectively.

For surface tension of the CaO–MgO–Al_2O_3–SiO_2–CaF_2–Na_2O system, Equation [1] can be expressed as Equations [2]–[7]:

$$\sigma = \sigma_{CaO}^{Pure} + \frac{RT}{A_{CaO}} ln \frac{N_{CaO}^{Surf}}{N_{CaO}^{Bulk}}; \quad [2]$$

$$\sigma = \sigma_{MgO}^{Pure} + \frac{RT}{A_{MgO}} ln \frac{N_{MgO}^{Surf}}{N_{MgO}^{Bulk}}; \quad [3]$$

$$\sigma = \sigma_{Al_2O_3}^{Pure} + \frac{RT}{A_{Al_2O_3}} ln \frac{N_{Al_2O_3}^{Surf}}{N_{Al_2O_3}^{Bulk}}; \quad [4]$$

$$\sigma = \sigma_{SiO_2}^{Pure} + \frac{RT}{A_{SiO_2}} ln \frac{N_{SiO_2}^{Surf}}{N_{SiO_2}^{Bulk}}; \quad [5]$$

$$\sigma = \sigma_{CaF_2}^{Pure} + \frac{RT}{A_{Na_2O}} ln \frac{N_{CaF_2}^{Surf}}{N_{CaF_2}^{Bulk}}; \quad [6]$$

$$\sigma = \sigma_{Na_2O}^{Pure} + \frac{RT}{A_{Na_2O}} ln \frac{N_{Na_2O}^{Surf}}{N_{Na_2O}^{Bulk}}; \quad [7]$$

where the molar volumes of the pure molten components (V_i) recommended by Mills et al. (2011) are used in the present model, as listed in Table I. The surface tension of pure component i is given by σ_i^{Pure}, and the equations for determining the temperature dependences of surface tension are listed in Table II (Mills et al., 2011; National Institute of Standards and Technology, 1987).

Based on the above description, the key points of the model for surface tension calculation are established from the mass action concentrations in the surface (N_i^{Surf}) and bulk (N_i^{Bulk}) for the CaO–MgO–Al_2O_3–SiO_2–CaF_2–Na_2O system. The mass action concentrations of the structures in the surface and bulk were calculated by the ion and molecule coexistence theory of slag structure and related diagrams (Slag Atlas, 1995; Zhang, 2001; Zhang, 2003) as follows:

- The structural units of the surface phase of the CaO–MgO–Al_2O_3–SiO_2–CaF_2–Na_2O system are the same as in the bulk phase of the molten slag, and composed of simple ions (Ca^{2+}, Mg^{2+}, Na^{2+}, O^{2-}, F^-), simple molecules (Al_2O_3, SiO_2), and complex molecules. At metallurgical temperatures, components such as CaO, MgO, CaF_2, and Na_2O in molten slag can dissociate to form simple ions. Components such as SiO_2 and Al_2O_3 in molten slag cannot be dissociated due to the predominance of covalent bonds, and thus exist in a molecular state or in the form of complex compounds. The structural units of this system are listed in Table III.
- There are dynamic equilibrium chemical reactions between simple ions, simple molecules, and complex molecules both in the surface and bulk layers.

Taking calcium silicate formation as an example:

$$2(Ca^{2+}+O^{2-}) + SiO_2 = 2CaO{\cdot}SiO_2. \quad [8]$$

Table I

Molar volumes of pure component (m³/mol)

Component	Temperature (K) dependence of molar volume (m³/mol)
CaO	$20.7 \times [1 + 1 \times 10^{-4} \times (T - 1773)] \times 10^{-6}$
MgO	$16.1 \times [1 + 1 \times 10^{-4} \times (T - 1773)] \times 10^{-6}$
Al_2O_3	$28.3 \times [1 + 1 \times 10^{-4} \times (T - 1773)] \times 10^{-6}$
SiO_2	$27.516 \times [1 + 1 \times 10^{-4} \times (T - 1773)] \times 10^{-6}$
CaF_2	$31.3 \times [1 + 1 \times 10^{-4} \times (T - 1773)] \times 10^{-6}$
Na_2O	$33.0 \times [1 + 1 \times 10^{-4} \times (T - 1773)] \times 10^{-6}$

Table II

Temperature dependences of surface tensions of pure components

Component	Temperature (K) dependence of surface tension (mN/m)
CaO	$791 - 0.0935T$
MgO	$1770 - 0.636T$
Al_2O_3	$1024 - 0.177T$
SiO_2	$243 + 0.031T$
CaF_2	$1604.6 - 0.72T$
Na_2O	$438 - 0.116T$

- There are dynamic equilibria between ions and molecules both in the surface and bulk layers. The chemical reactions and their thermodynamic parameters are given in Table III (Bale et al., 2002; Turkdogan, 1980; Wu et al., 2014).
- Chemical reactions in molten slags obey the Law of Mass Action in both the surface and bulk layers. Equation [9] can be applied:

$$K_{2CaO{\cdot}SiO2}^{\theta} = \frac{N_{2CaO{\cdot}SiO2}^{Sulf}}{\left(N_{CaO}^{Surf}\right)^2 \cdot \left(N_{SiO2}^{Sulf}\right)} = \frac{N_{2CaO{\cdot}SiO2}^{Bulk}}{\left(N_{CaO}^{Bulk}\right)^2 \cdot \left(N_{SiO2}^{Bulk}\right)} = \exp\left(-\frac{\Delta G^{\theta}}{RT}\right), \quad [9]$$

where $K_{2CaO{\cdot}SiO2}^{\theta}$ is the chemical reaction equilibrium constant of Equation [9], and can be calculated from ΔG^{θ}. The surface mass action concentrations depicted by $N_{2CaO{\cdot}SiO2}^{Sulf}$, N_{CaO}^{Sulf}, and N_{SiO2}^{Sulf} are those of $2CaO{\cdot}SiO_2$, ion couples (Ca^{2+} + O^{2-}), and SiO_2, respectively; the respective corresponding bulk mass action concentrations are given by $N_{2CaO{\cdot}SiO2}^{Bulk}$, N_{CaO}^{Bulk}, and N_{SiO2}^{Bulk}.

The mass action concentrations of the structural unit are defined as the ratio of the equilibrium mole number of structural unit i to the total equilibrium mole numbers of all structural units, calculated by $N_i = n_i / \sum n_i$. The mole numbers of CaO, MgO, Al_2O_3, SiO_2, CaF_2, and Na_2O in 100 g of total slag mass are defined as $b_1 = n_{CaO}$, $b_2 = n_{MgO}$, $b_3 = n_{CaF2}$, $b_4 = n_{Na2O}$, $a_1 = n_{Al2O3}$, and $a_2 = n_{SiO2}$, respectively. The symbols of the mass action concentrations for all structural units are listed as follows: $N_1 = N_{CaO}$, $N_2 = N_{MgO}$, $N_3 = N_{Al2O3}$, $N_4 = N_{SiO2}$, $N_5 = N_{CaF2}$, $N_6 = N_{Na2O}$. Mass equilibria formulae for the CaO–MgO–Al_2O_3–SiO_2–CaF_2–Na_2O system are given by Equations [10]–[16]:

Table III

Expression of structural units, standard Gibbs free energies chemical reactions of complex molecules, their standard Gibbs free energies, and mass action concentrations of CaO–MgO–Al_2O_3–SiO_2–CaF_2–Na_2O slag system

	Structural unit	Reaction	$\Delta G\theta$ (J·mol^{-1})	Mass action concentration
Simple ions	$Ca^{2+}+O^{2-}$			N_1
	$Mg^{2+}+O^{2-}$			N_2
	$2Na^{2+}+O^{2-}$			N_5
	$Ca^{2+}+2F^{-}$			N_6
Simple molecules	Al_2O_3			N_3
	SiO_2			N_4
Complex molecules	$2MgO·SiO_2$	$2(Mg^{2+}+O^{2-})+SiO_2 \leftrightarrow 2MgO·SiO_2$	$-77\,403+11.0T$	$N_7=K_1^{\theta}·N_2^2·N_4$
	$MgO·SiO_2$	$(Mg^{2+}+O^{2-})+SiO_2 \leftrightarrow MgO·SiO_2$	$43\,400-40.0T$	$N_8=K_2^{\theta}·N_2·N_4$
	$2CaO·SiO_2$	$2(Ca^{2+}+O^{2-})+SiO_2 \leftrightarrow 2CaO·SiO_2$	$-100\,986-24.03T$	$N_9=K_3^{\theta}·N_1^2·N_4$
	$CaO·SiO_2$	$(Ca^{2+}+O^{2-})+SiO_2 \leftrightarrow CaO·SiO_2$	$-22\,476-38.52T$	$N_{10}=K_4^{\theta}·N_1·N_4$
	$3CaO·2SiO_2$	$3(Ca^{2+}+O^{2-})+2SiO_2 \leftrightarrow 3CaO·2SiO_2$	$-258\,102-0.317T$	$N_{11}=K_5^{\theta}·N_1^3·N_4^2$
	$3CaO·SiO_2$	$3(Ca^{2+}+O^{2-})+SiO_2 \leftrightarrow 3CaO·SiO_2$	$-138\,462-26.732T$	$N_{12}=K_6^{\theta}·N_1^3·N_4$
	$3Al_2O_3·2SiO_2$	$3Al_2O_3+2SiO_2 \leftrightarrow 3Al_2O_3·2SiO_2$	$18\,935-27.009T$	$N_{13}=K_7^{\theta}·N_3^3·N_4^2$
	$Al_2O_3·SiO_2$	$Al_2O_3+SiO_2 \leftrightarrow Al_2O_3·SiO_2$	$-102\,686-9.094T$	$N_{14}=K_8^{\theta}·N_3·N_4$
	$CaO·Al_2O_3$	$(Ca^{2+}+O^{2-})+Al_2O_3 \leftrightarrow CaO·Al_2O_3$	$-20\,123-19.089T$	$N_{15}=K_9^{\theta}·N_1·N_3$
	$12CaO·7Al_2O_3$	$12(Ca^{2+}+O^{2-})+7Al_2O_3 \leftrightarrow 12CaO·7Al_2O_3$	$-86\,100-205.1T$	$N_{16}=K_{10}^{\theta}·N_1^{12}·N_3^7$
	$3CaO·Al_2O_3$	$3(Ca^{2+}+O^{2-})+Al_2O_3 \leftrightarrow 3CaO·Al_2O_3$	$-1716-45.309T$	$N_{17}=K_{11}^{\theta}·N_1^3·N_3$
	$2CaO·Al_2O_3$	$2(Ca^{2+}+O^{2-})+Al_2O_3 \leftrightarrow 2CaO·Al_2O_3$	$-5447-6.050T$	$N_{18}=K_{12}^{\theta}·N_1^2·N_3$
	$CaO·2Al_2O_3$	$(Ca^{2+}+O^{2-})+2Al_2O_3 \leftrightarrow CaO·2Al_2O_3$	$-22\,902-28.486T$	$N_{19}=K_{13}^{\theta}·N_1·N_3^2$
	$CaO·6Al_2O_3$	$(Ca^{2+}+O^{2-})+6Al_2O_3 \leftrightarrow CaO·6Al_2O_3$	$-8721-56.572T$	$N_{20}=K_{14}^{\theta}·N_1·N_3^6$
	$2CaO·Al_2O_3·SiO_2$	$2(Ca^{2+}+O^{2-})+Al_2O_3+SiO_2 \leftrightarrow 2CaO·Al_2O_3·SiO_2$	$-137\,321-39.317T$	$N_{21}=K_{15}^{\theta}·N_1^2·N_3·N_4$
	$CaO·Al_2O_3·2SiO_2$	$(Ca^{2+}+O^{2-})+Al_2O_3+2SiO_2 \leftrightarrow CaO·Al_2O_3·2SiO_2$	$-87\,988-31.419T$	$N_{22}=K_{16}^{\theta}·N_1·N_3·N_4^2$
	$CaO·Al_2O_3·SiO_2$	$(Ca^{2+}+O^{2-})+Al_2O_3+SiO_2 \leftrightarrow CaO·Al_2O_3·SiO_2$	$-66387-22.869T$	$N_{23}=K_{17}^{\theta}·N_1·N_3·N_4$
	$3CaO·Al_2O_3·3SiO_2$	$3(Ca^{2+}+O^{2-})+Al_2O_3+3SiO_2 \leftrightarrow 3CaO·Al_2O_3·3SiO_2$	$-337\,740+58.262T$	$N_{24}=K_{18}^{\theta}·N_1^3·N_3·N_4^3$
	$CaO·MgO·SiO_2$	$(Ca^{2+}+O^{2-})+(Mg^{2+}+O^{2-})+SiO_2 \leftrightarrow CaO·MgO·SiO_2$	$-108248-7.595T$	$N_{25}=K_{19}^{\theta}·N_1·N_2·N_4$
	$3CaO·MgO·2SiO_2$	$3(Ca^{2+}+O^{2-})+(Mg^{2+}+O^{2-})+2SiO_2 \leftrightarrow 3CaO·MgO·2SiO_2$	$-243\,680-25.218T$	$N_{26}=K_{20}^{\theta}·N_1^3·N_2·N_4^2$
	$CaO·MgO·2SiO_2$	$(Ca^{2+}+O^{2-})+(Mg^{2+}+O^{2-})+2SiO_2 \leftrightarrow CaO·MgO·2SiO_2$	$-8685-78.716T$	$N_{27}=K_{21}^{\theta}·N_1·N_2·N_4^2$
	$2CaO·MgO·2SiO_2$	$2(Ca^{2+}+O^{2-})+(Mg^{2+}+O^{2-})+2SiO_2 \leftrightarrow 2CaO·MgO·2SiO_2$	$-186\,446-15.933T$	$N_{28}=K_{22}^{\theta}·N_1^2·N_2·N_4^2$
	$MgO·Al_2O_3$	$(Mg^{2+}+O^{2-})+Al_2O_3 \leftrightarrow MgO·Al_2O_3$	$-15\,606-15.034T$	$N_{29}=K_{23}^{\theta}·N_2·N_3$
	$CaO·MgO$	$(Ca^{2+}+O^{2-})+(Mg^{2+}+O^{2-}) \leftrightarrow CaO·MgO$	$-5708-2.570T$	$N_{30}=K_{24}^{\theta}·N_1·N_2$
	$7MgO·9Al_2O_3·3SiO_2$	$7(Mg^{2+}+O^{2-})+9Al_2O_3+3SiO_2 \leftrightarrow 7MgO·9Al_2O_3·3SiO_2$	$-160\,781+7.180T$	$N_{31}=K_{25}^{\theta}·N_2^7·N_3^9·N_4^3$
	$2MgO·2Al_2O_3·5SiO_2$	$2(Mg^{2+}+O^{2-})+2Al_2O_3+5SiO_2 \leftrightarrow 2MgO·2Al_2O_3·5SiO_2$	$-68\,380-19.294T$	$N_{32}=K_{26}^{\theta}·N_2^2·N_3^2·N_4^5$
	$3MgO·Al_2O_3·3SiO_2$	$3(Mg^{2+}+O^{2-})+Al_2O_3+3SiO_2 \leftrightarrow 3MgO·Al_2O_3·3SiO_2$	$198\,027-163.550T$	$N_{33}=K_{27}^{\theta}·N_2^3·N_3·N_4^3$
	$3CaO·3Al_2O_3·CaF_2$	$3(Ca^{2+}+O^{2-})+3Al_2O_3+(Ca^{2+}+2F^{-}) \leftrightarrow 3CaO·3Al_2O_3·CaF_2$	$-44\,492-73.15T$	$N_{34}=K_{28}^{\theta}·N_1^3·N_3^3·N_5$
	$11CaO·7Al_2O_3·CaF_2$	$11(Ca^{2+}+O^{2-})+7Al_2O_3+(Ca^{2+}+2F^{-}) \leftrightarrow 11CaO·7Al_2O_3·CaF_2$	$-228\,760-155.8T$	$N_{35}=K_{29}^{\theta}·N_1^{11}·N_3^7·N_5$
	$3CaO·2SiO_2·CaF_2$	$3(Ca^{2+}+O^{2-})+2SiO_2+(Ca^{2+}+2F^{-}) \leftrightarrow 3CaO·2SiO_2·CaF_2$	$-205\,169.8-27.66T$	$N_{36}=K_{30}^{\theta}·N_1^3·N_4^2·N_5$
	$2Na_2O·SiO_2$	$2(2Na^{2+}+O^{2-})+SiO_2 \leftrightarrow 2Na_2O·SiO_2$	$-517\,220.2+124.22T$	$N_{37}=K_{31}^{\theta}·N_4·N_6^2$
	$Na_2O·SiO_2$	$(2Na^{2+}+O^{2-})+SiO_2 \leftrightarrow Na_2O·SiO_2$	$-299\,348.7+55.32T$	$N_{38}=K_{32}^{\theta}·N_4·N_6$
	$Na_2O·2SiO_2$	$(2Na^{2+}+O^{2-})+2SiO_2 \leftrightarrow Na_2O·2SiO_2$	$-279\,093.8+23.19T$	$N_{39}=K_{33}^{\theta}·N_4^2·N_6$
	$Na_2O·Al_2O_3$	$(2Na^{2+}+O^{2-})+Al_2O_3 \leftrightarrow Na_2O·Al_2O_3$	$-247\,970.8+44.6T$	$N_{40}=K_{34}·N_3·N_6$
	$Na_2O·3Al_2O_3$	$(2Na^{2+}+O^{2-})+3Al_2O_3 \leftrightarrow Na_2O·3Al_2O_3$	$-282\,626.4+35.28T$	$N_{41}=K_{35}·N_3^3·N_6$
	$Na_2O·6Al_2O_3$	$(2Na^{2+}+O^{2-})+6Al_2O_3 \leftrightarrow Na_2O·6Al_2O_3$	$-283\,433.47+35.76T$	$N_{42}=K_{36}·N_3^6·N_6$
	$Na_2O·9Al_2O_3$	$(2Na^{2+}+O^{2-})+9Al_2O_3 \leftrightarrow Na_2O·9Al_2O_3$	$-295\,918+25.18T$	$N_{43}=K_{37}·N_3^9·N_6$
	$Na_2O·Al_2O_3·2SiO_2$	$(2Na^{2+}+O^{2-})+Al_2O_3+2SiO_2 \leftrightarrow Na_2O·Al_2O_3·2SiO_2$	$-370\,572.02+9.98T$	$N_{44}=K_{38}·N_3·N_4^2·N_6$
	$Na_2O·Al_2O_3·4SiO_2$	$(2Na^{2+}+O^{2-})+Al_2O_3+4SiO_2 \leftrightarrow Na_2O·Al_2O_3·4SiO_2$	$-44\,0859.8+101.36T$	$N_{45}=K_{39}N_3·N_4^4·N_6·$
	$Na_2O·Al_2O_3·6SiO_2$	$(2Na^{2+}+O^{2-})+Al_2O_3+6SiO_2 \leftrightarrow Na_2O·Al_2O_3·6SiO_2$	$-425\,604+19.38T$	$N_{46}=K_{40}·N_3·N_4^6·N_6$
	$Na_2O·2Al_2O_3·3SiO_2$	$(2Na^{2+}+O^{2-})+2Al_2O_3+3SiO_2 \leftrightarrow Na_2O·2Al_2O_3·3SiO_2$	$-609\,393.42+126.91T$	$N_{47}=K_{41}·N_3^2·N_4^3·N_6$
	$2Na_2O·CaO·3SiO_2$	$2(2Na^{2+}+O^{2-})+(Ca^{2+}+O^{2-})+3SiO_2 \leftrightarrow 2Na_2O·CaO·3SiO_2$	$-672\,019.9+62.8T$	$N_{48}=K_{42}·N_1·N_4^3·N_6^2$
	$Na_2O·CaO·5SiO_2$	$(2Na^{2+}+O^{2-})+(Ca^{2+}+O^{2-})+5SiO_2 \leftrightarrow Na_2O·CaO·5SiO_2$	$-443\,841.2+63.84T$	$N_{49}=K_{43}·N_1·N_4^5·N_6$
	$Na_2O·2CaO·3SiO_2$	$(2Na^{2+}+O^{2-})+2(Ca^{2+}+O^{2-})+3SiO_2 \leftrightarrow Na_2O·2CaO·3SiO_2$	$-607\,292.6+125.68T$	$N_{50}=K_{44}·N_1^2·N_4^3·N_6$
	$Na_2O·3CaO·6SiO_2$	$(2Na^{2+}+O^{2-})+3(Ca^{2+}+O^{2-})+6SiO_2 \leftrightarrow Na_2O·3CaO·6SiO_2$	$-837\,543.4+219.73T$	$N_{51}=K_{45}·N_1^3·N_4^6·N_6$
	$Na_2O·MgO·4SiO_2$	$(2Na^{2+}+O^{2-})+(Mg^{2+}+O^{2-})+4SiO_2 \leftrightarrow Na_2O·MgO·4SiO_2$	$-306\,210.4-1.2T$	$N_{52}=K_{46}·N_2·N_4^4·N_6$
	$Na_2O·2MgO·6SiO_2$	$(2Na^{2+}+O^{2-})+2(Mg^{2+}+O^{2-})+6SiO_2 \leftrightarrow Na_2O·2MgO·6SiO_2$	$-312\,061.3-33.06T$	$N_{53}=K_{47}·N_2^2·N_4^6·N_6$

$$b_1 = \Sigma n_i(0.5N_1 + 3N_9 + N_{10} + 3N_{11} + 3N_{12} + N_{15} + 12N_{16} + 3N_{17} + 2N_{18} + N_{19} + N_{20} + 2N_{21} + N_{22} + N_{23} + 3N_{24} + N_{25} + 3N_{26} + N_{27} + 2N_{28} + N_{30} + 3N_{34} + 11N_{35} + 3N_{36} + N_{48} + N_{49} + 2N_{50} + 3N_{51}); \quad [10]$$

$$b_2 = \Sigma n_i(0.5N_2 + 2N_7 + N_8 + N_{25} + N_{26} + N_{27} + N_{28} + N_{29} + N_{30} + 7N_{31} + 2N_{32} + 3N_{33} + 2N_{52} + 2N_{53}); \quad [11]$$

$$b_3 = \Sigma n_i(0.33N_5 + N_{34} + N_{35} + N_{36}); \quad [12]$$

$$b_4 = \Sigma n_i(0.33N_6 + 2N_{37} + N_{38} + N_{39} + N_{40} + N_{41} + N_{42} + N_{43} + N_{44} + N_{45} + N_{46} + N_{47} + 2N_{48} + N_{49} + N_{50} + N_{51} + N_{52} + N_{53}); \quad [13]$$

$$a_1 = \Sigma n_i(N_3 + 3N_{13} + N_{14} + N_{15} + 7N_{16} + N_{17} + N_{18} + 2N_{19} + 6N_{20} + N_{21} + N_{22} + N_{23} + N_{24} + N_{29} + 9N_{31} + 2N_{32} + N_{33} + 3N_{34} + 7N_{35} + N_{40} + 3N_{41} + 6N_{42} + 9N_{43} + N_{44} + N_{45} + N_{46} + 2N_{47}); \quad [14]$$

$$a_2 = \Sigma n_i(N_4 + N_7 + N_8 + N_9 + N_{10} + 2N_{11} + N_{12} + 2N_{13} + N_{14} + N_{21} + 2N_{22} + N_{23} + 3N_{24} + N_{25} + 2N_{26} + 2N_{27} + 2N_{28} + 3N_{31} + 5N_{32} + 3N_{33} + 2N_{36} + N_{37} + N_{38} + 2N_{39} + 2N_{44} + 4N_{45} + 6N_{46} + 3N_{47} + 3N_{48} + 5N_{49} + 3N_{50} + 6N_{51} + 4N_{52} + 6N_{53}); \quad [15]$$

$$\Sigma N_i = 1 \quad [16]$$

Therefore, Equations [10]–[16] are the governing equations of the developed thermodynamic model for calculating mass action concentrations N_i of structural units or ion couples in the CaO–MgO–Al_2O_3–SiO_2–CaF_2–Na_2O system for a certain temperature and components, where N_7–N_{53} can be represented by N_1–N_6.

- The relationship between surface tension of a melt system and mass action concentrations of surface and bulk components conforms to Butler's equation. The process to estimate the surface tension model is shown in Figure 1; detailed discussions of this method are given by Cheng and Liao (1999) and Xu et al. (2017). For a given slag chemical composition x_i and temperature T, the K_i^θ reaction equilibrium constant can be calculated, and then the mass action concentrations in the bulk (N_i^{Bulk}) can be calculated from the mole fractions of the components and the chemical reaction equilibria constants of complex molecules based on the ion and molecule coexistence theory. Surface tension (σ) and the mass action concentrations in the surface (N_i^{Sur}) can be calculated from N_i^{Bulk}, σ_i^{Pure}, and A_i based on this theory and Butler's equation.

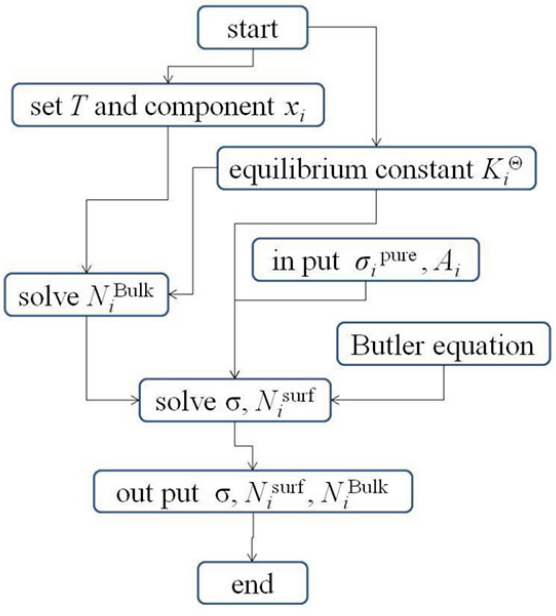

Figure 1—Estimation process for surface tension model

Results and discussion

Comparison between estimated values and experimental data

Comparison between the estimated surface tension values and those measured, as reported from the literature, for the CaO–MgO–Al_2O_3–SiO_2–CaF_2–Na_2O related system is shown in Figure 2. The average error (Δ) of all calculated values can be assessed using Equation [17], where the Δ(%) value is calculated by taking the summation of the percentage differences of the calculated and measured values and dividing by the number of data points:

$$\Delta(\%) = \frac{1}{N}\sum_{n=1}^{N}\left|\frac{\sigma_{cal} - \sigma_{exp}}{\sigma_{cal}}\right| \times 100. \quad [17]$$

The estimated values using this model were compared with experimental data to verify the model. The result indicated that the estimated values agree with the experimental data (Dou et al., 2009; Slag Atlas, 1995). For all calculated values, the average error Δ(%) is 8.19%. The detailed average errors for related experimental systems are also shown in Table IV. The average error Δ(%) for the MgO–Al_2O_3–SiO_2–CaF_2 system is about 12.67%, which could be related to the slag composition, which has high CaF_2 content and no CaO. The deviation of individual points is also relatively large in the CaO–Al_2O_3–SiO_2–CaF_2–Na_2O system. The larger experimental measurements may be related to the fact that the slag may be in a non-homogeneous region due to its lower basicity (~ 0.45) owing to low CaF_2 and Al_2O_3 contents. The model prediction achieved reasonable accuracy of surface tension variation in the fully liquid phase of the CaO–MgO–Al_2O_3–SiO_2–CaF_2–Na_2O system and its sub-systems.

Surface tension of CaO–SiO_2-based mold flux

Traditional mold flux is based on the CaO–SiO_2 system, which has low basicity (CaO/SiO_2 mass ratio) and low viscosity, to which fluxing agents such as CaF_2, Na_2O, and B_2O_3 are added to optimize

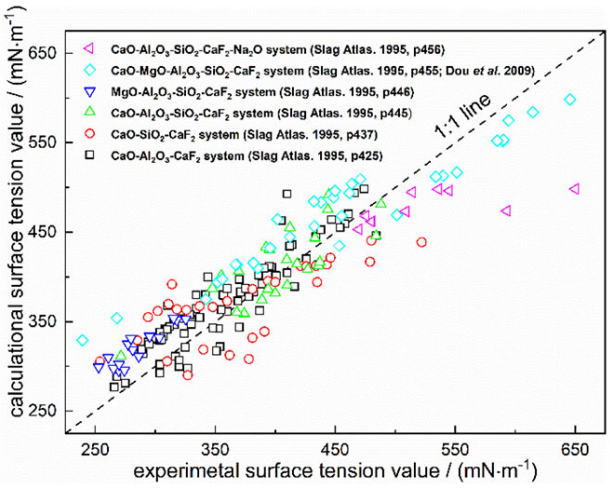

Figure 2—Comparison between calculated values with measured values for related systems

Table IV

Composition, temperature, and relative average errors for related experimental systems

System	Composition range (mass%)						Temperature range (K)	Average error (%)
	CaO	MgO	Al_2O_3	SiO_2	CaF_2	Na_2O		
$CaO–Al_2O_3–CaF_2$	0–700		–60		7–96		1773–1873	6.38
$CaO–SiO_2–CaF2$	0–70			0–60	0–93		1773	10.44
$CaO–Al_2O_3–SiO_2–CaF_2$	2–50		2–45	1–30	5–67		1773	6.40
$MgO–Al_2O_3–SiO_2–CaF_2$		0–40	10–50	0–20	30–50		1873	12.67
$CaO–MgO–Al_2O_3–SiO_2–CaF_2$	21–58	3–24	3–39	2–24	0–52		1773–1873	9.67
$CaO–Al_2O_3–SiO_2–CaF_2–Na_2O$	20–40		10	25–45	0–20	5	1873	8.79
Average								8.19

the properties. The surface tension of the $CaO–SiO_2–CaF_2$ system was evaluated, and the calculated results are shown in Figure 3. The four lines in this figure indicate the calculated results for the iso-surface tensions at 330, 360, 390, and 420 mN/m. Figure 3 also shows the boundary of the homogeneous region at 1773 K, calculated using the thermodynamic software FACTSAGE. The result indicates that both CaF_2 content and basicity influence the surface tension. When the CaF_2 content was lower than 20%, the effects of basicity and CaF_2 addition on the surface tension were similar; when the CaF_2 content was higher than 20%, the basicity had a more significant effect. Figure 4(a) shows the effect of basicity with different Al_2O_3 contents on the surface tension at 1773 K. The results indicate that the surface tension increased with increase of basicity. The trends of surface tension effected by the Al_2O_3 content and basicity were the same. Figure 4(b) shows the effect of the CaF_2 content with different Na_2O contents on the surface tension at 1773 K. The surface tension decreased with increase of CaF_2 content. The trends of surface tension effected by Na_2O content and CaF_2 content were also the same, although Na_2O had a more significant effect.

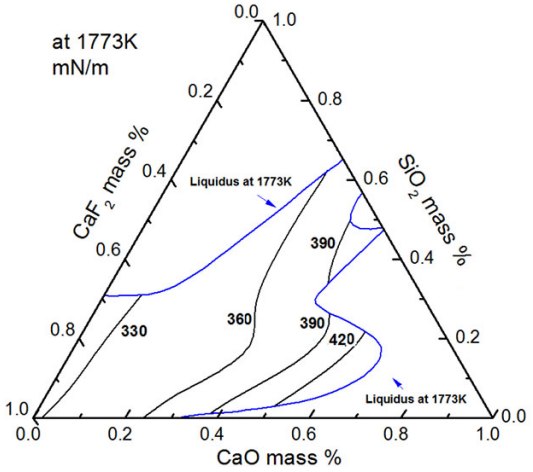

Figure 3—Calculated iso-surface tension lines of molten $CaO–SiO_2–CaF_2$ system at 1773 K

Surface tension of $CaO–Al_2O_3$-based mold flux

The newly developed $CaO–Al_2O_3$-based mold flux has a high Al_2O_3 content and relatively low SiO_2 content. This flux shows strong potential for application to continuous casting (Wang et al., 2016). Surface tension of the $CaO–Al_2O_3–CaF_2$ system was also evaluated, and the calculated results are shown in Figure 5. The five lines in this figure indicate the calculated results for the iso-surface tensions at 360, 390, 420, 450, and 480 mN/m. The boundary of the homogenous phase region at 1773 K, calculated using the thermodynamic software FACTSAGE, is also shown. The surface tension value of the $CaO–Al_2O_3$-based mold flux is larger than that of the $CaO–SiO_2$-based mold flux. The result also indicates that the surface tension significantly decreased with increase of CaF_2 content. The effects of CaO and Al_2O_3 contents on surface tension

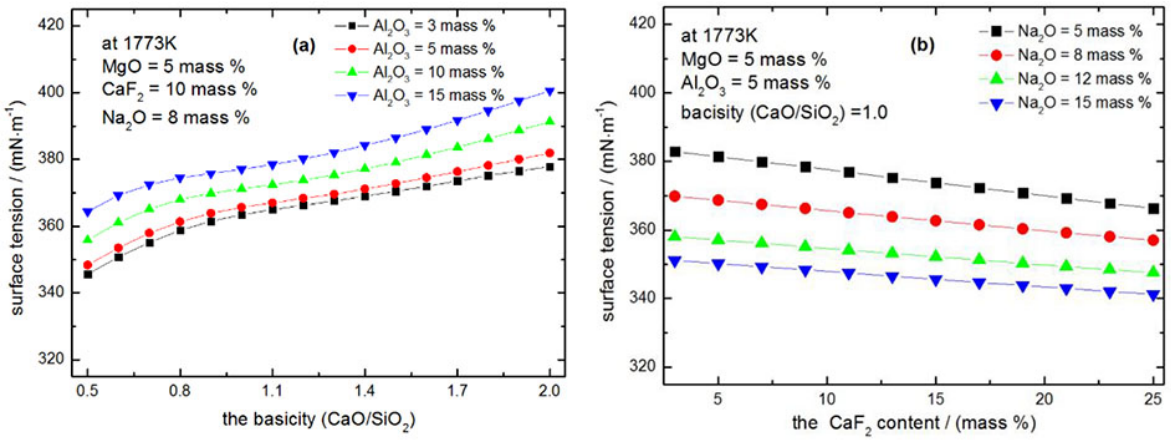

Figure 4—Relationships between surface tension of $CaO–SiO_2$-based mold flux with composition. (a) Basicity and Al_2O_3 content, (b) CaF_2 content and Na_2O content

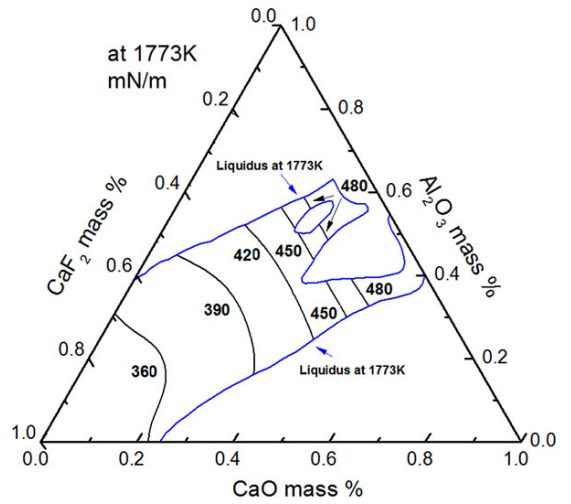

Figure 5—Calculated iso-surface tension lines of molten CaO–Al_2O_3–CaF_2 system at 1773 K

are not significant for a given CaF_2 content. CaF_2 addition has a more significant effect on surface tension than the mass ratio of CaO/Al_2O_3. Figure 6(a) shows the effect of the CaO/Al_2O_3 mass ratio for different SiO_2 contents on the surface tension at 1773 K. With increase of the CaO/Al_2O_3 mass ratio, the surface tension decreased with increase of SiO_2 content. For the same SiO_2 content, the surface tension slowly increased with increase in the CaO/Al_2O_3 mass ratio. Figure 6(b) shows the effect of CaF_2 content for different Na_2O contents on the surface tension at 1773 K. The surface tension significantly decreased with CaF_2 content, more strongly than that in the CaO–SiO_2-based mold flux. The trend of change of surface tension with Na_2O content was the same as that of CaF_2 content, but CaF_2 had a more significant effect.

These results confirm other reports (Mills et al., 2011) that the surface-active components (SiO_2, CaF_2, and Na_2O) preferentially migrate to the surface and cause a sharp decrease in surface tension. In general, on the basis of the additive method widely used for alloys and slags, surface tension of slag depends on the surface tension of the oxides (Mills, 1993). The surface tensions of CaO, MgO, Al_2O_3, SiO_2, CaF_2, and Na_2O pure components are 625, 642, 710, 298, 32,8 and 232 mN/m at 1773 K, respectively (Hanao et al., 2007). Because the surface tensions of pure SiO_2, CaF_2, and Na_2O are much lower than those of CaO, MgO, and Al_2O_3, surface tension of mold flux will decrease with small increases in SiO_2, CaF_2, and Na_2O contents. For instance, with increasing basicity of the CaO–SiO_2-based mold flux, the SiO_2 content will reduce, which could lead to an increase in the slag surface tension. With increasing CaO/Al_2O_3 mass ratio in the CaO–Al_2O_3-based mold flux, the content of surface-active components is only slightly reduced and surface tension slowly increases.

Conclusions

- A thermodynamic model for determining the surface tension of mold flux slag containing fluoride was developed based on the ion and molecule coexistence theory of slag structure and Butler's equation. The results indicated that the surface tension model could fit the experimental data well.
- Surface tension of the CaO–Al_2O_3-based mold flux is larger than that of the CaO–SiO_2-based mold flux. The surface tension in a multi-component system decreased with increasing content of surface-active components: SiO_2, CaF_2, and Na_2O. This effect was more significant in the CaO–Al_2O_3-based mold flux.
- In the CaO–SiO_2-based system, the surface tension increased with increasing basicity and Al_2O_3 content. In the CaO–Al_2O_3-based system, the surface tension slowly increased with increasing CaO/Al_2O_3 mass ratio and decreased with increasing SiO_2 content.

Acknowledgements

This work was supported by Project no. 51704201, sponsored by the National Natural Science Foundation of China. English editing of this manuscript was carried by Kathryn C. Sole (PhD).

References

Aune, R., Hayashi, M., Nakajima, K., Seetharaman, S. 2002. Thermophysical properties of silicate slags. *JOM*, vol. 54, no. 11, pp. 62–69.

Bale, C.W., Chamand, P., Degterov, S.A., Erkseon, G., Hack, K., Ben Mehfoud, R., Melancan, J., Pelton, A.D., Petetaen, S. 2002. FactSage thermochemical software and databases. *Calphad*, vol, 26, no. 2, pp.189–228.

Butler, J.A.V. 1932. The thermodynamics of the surfaces of solutions. *Proceedings of the Royal Society of London Series A*, vol. 135, pp. 348–375.

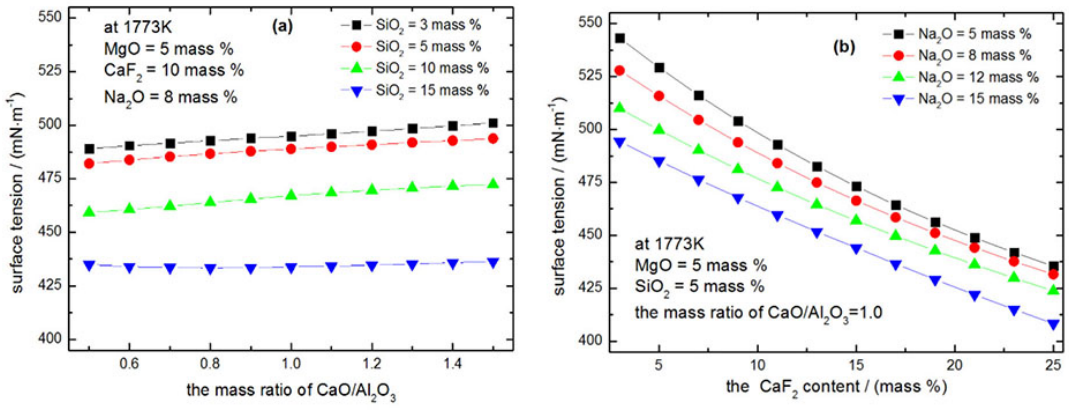

Figure 6— Relationship between surface tension of CaO–Al_2O_3-based mold flux with composition. (a) CaO/Al_2O_3 mass ratio and SiO_2 content, (b) CaF_2 content and Na_2O content

Cheng, G.G., Liao, N.B. 1999. Calculation model for surface tension of slag melt. *Journal of Iron and Steel Research International*, vol. 6, no. 2, pp. 17–20.

Chou, K.C., Zhang, G.H. 2009. Calculation of physicochemical properties with limited discrete data in multicomponent systems. *Materials Transactions B*, vol. 40, no. 2, pp. 223–232.

Dong, Y.W., Jiang, Z.H., Cao, Y.Y., Zhang, H.K., Shen, H.J. 2014. Effect of MgO and SiO_2 on surface tension of fluoride containing slag. *Journal of Central South University*, vol. 21, no. 11, pp. 4104–4108.

Dou, Z.H., Zhang, T.A., Yao, J.M., Niu, L.P., Jiang, X.L., He, J.C. 2009. Research on properties of CaF_2–CaO–Al_2O_3–MgO–SiO_2 refining slag. *Chinese Journal of Process Engineering*, vol. 9, no. S1, pp. 132–136 [in Chinese].

Hanao, M., Tanaka, T., Kawamoto, M., Takatani, K. 2007. Evaluation of surface tension of molten slag in multi-component systems. *ISIJ International*, vol. 47, no. 7, pp. 935–939.

Mills, K.C. 1993. The influence of structure on the physico-chemical properties of slags. *ISIJ Inernational*, vol. 33, no. 1, pp. 148–155.

Mills, K.C., Fox, A.B., Li, Z., Thackray, R.P. 2005. Performance and properties of mould fluxes. *Ironmaking and Steelmaking*, vol. 32, no. 1, pp. 26–34.

Mills, K.C., Yuan, L., Jones, R.T. 2011, Estimating the physical properties of slags. *Journal of the Southern African Institute of Mining and Metallurgy*, vol. 111, no. 10, pp. 649–658.

National Institute of Standards and Technology. 1987. *NIST Molten Salt Database.* National Institute of Standards and Technology, New York.

Qiao, Z.Y., Yan, L.J., Cao, Z.M., Xie, Y.N. 2001. Surface tension prediction of high-temperature melts. *Journal of Alloys and Compounds*, vol. 325, no. 1–2, pp. 180–189.

Slag Atlas. 1995. 2nd edn., Verlag Stahleisen, Düsseldorf. p. 425, p. 437, p. 445, p. 446, p. 455, p. 456.

Turkdogan, E.T. 1980. P*hysical Chemistry of High Temperature Technology*. Academic Press Inc, New York.

Wang, W.L., Li, J.G., Zhou, L.U., Yang, J. 2016. Effect of MnO content on the interfacial property of mold flux and steel. *Metals and Materials International*, vol. 22, no. 4, pp. 700–706.

Wang, W.L., Lu B.X., Xiao, D. 2016. A review of mold flux development for the casting of high-Al steels. *Materials Transactions B*, vol. 47, no. 1, pp. 384–389.

Wu, C.C., Cheng, G.G., Ma, Q.Q. 2014. Calculating model on the surface tension of CaF_2–CaO–Al_2O_3–MgO–SiO_2 slag system. *Shanghai Metals*, vol. 36, no. 3, pp. 33–36 [in Chinese].

Xu, J.F., Zhang, J.Y., Chen, D., Sheng, M.Q., Weng, W.P. 2016. Effects of MgO content and CaO/Al_2O_3 ratio on surface tension of calcium aluminate refining slag. *Journal of Central South University*, vol. 23, no. 12, pp. 3079–3084.

Xu, J.F., Li, J.C., Weng, W.P., Sheng, M.Q., Chen, D., Zhang, J.Y., Chen, Y. 2017. Calculation of surface tension for MgO–B_2O_3–SiO_2–CaO–Al_2O_3 molten boron-rich slag system. *Chinese Journal of Nonferrous Metals*, vol. 27, no. 1, pp. 206–214 [in Chinese].

Zhang, J. 2001. The application of the law of mass action in combination with the coexistence theory of slag structure to the multicomponent slag systems. *Acta Metallurgica Sinica* (English Edition), vol. 14, no. 3, pp. 177–190.

Zhang, J. 2003. Coexistence theory of slag structure and its application to calculation of oxidizing capability of slag melts. *Journal of Iron and Steel Research, International*, vol. 10, no. 1, pp. 1–10.

Zhang, J.Y., Shu, Q.F., Wei, S.K. 2003, Prediction of surface tension in molten metallic and ionic systems. *High Temperature Materials and Processes*, vol. 22, no. 5–6, pp. 395–400. ◆